Ultrasonics 49 (2009) 149–152

Contents lists available at ScienceDirect

Ultrasonics

journal homepage: www.elsevier.com/locate/ultras

Short Communication

Thickness vibration of piezoelectric plates of 6 mm crystals with tilted six-fold axis and two-layered thick electrodes

Jianke Du [a], Kai Xian [a], Ji Wang [a], Jiashi Yang [a,b,*]

[a] Mechanics and Materials Science Research Center, School of Engineering, Ningbo University, 818 Fenghua Road, Ningbo, Zhejiang 315211, China
[b] Department of Engineering Mechanics, University of Nebraska, Lincoln, NE 68588-0526, USA

ARTICLE INFO

Article history:
Received 9 April 2008
Received in revised form 11 September 2008
Accepted 15 September 2008
Available online 21 September 2008

Keywords:
Piezoelectricity
Plate
Vibration

ABSTRACT

We perform a theoretical analysis of thickness vibrations in piezoelectric plates of crystals with 6 mm symmetry. The six-fold axis is tilted with respect to the plate surfaces. The major surfaces of the plate are covered with two layers of electrodes of different metals. The equations of linear piezoelectricity are used for the crystal plate. The electrodes are modeled by the equations of elasticity. Thickness vibrations frequencies and modes as well as impedance are calculated and examined.

1. Introduction

Aluminum nitride (AlN) and zinc oxide (ZnO) both belong to crystals of 6 mm symmetry. Thin AlN and ZnO plates are of current and growing research interest because of the development of thin film bulk acoustic wave resonators (FBAR), e.g., [1–5]. AlN and ZnO plates with the six-fold axis normal, in-plane or tilted [3] with respected to the plate surfaces are all being developed. These plates can be either mounted to a substrate or lifted [1]. They have great potential for new devices. Thickness vibration modes are basic modes for device operation. There have been theoretical analyses on thickness vibrations of these plates, e.g., [5]. In these existing analyses, the electrodes are assumed to be very thin such that they only provide an electrical constraint on the electric potential, but their mechanical effects like stiffness and inertia are neglected. While the thin-electrode approximation is often used in the analysis of basic resonator vibration characteristics, sometimes the effects of electrode stiffness or inertia need to be considered. This is especially true for FBARs because they are made of very thin crystal plates and therefore the mechanical effects of the electrodes are more pronounced. In [6] the effects of single-layered thick electrodes were considered theoretically and experimentally. However, more general than what was analysed in [6], in resonator manufacturing, two layers of metals are often used for electrodes to achieve optimal adhesion to the crystal plate and electronic conduction [3]. This electrode fine feature also needs to be taken into account for an accurate description of FBARs. Another effect that we want to take into consideration is that when a resonator is being made, one side of the plate is pre-deposited with an electrode of known thickness, and then the thickness of the electrode on the other side of the plate is determined by that the electroded resonator has a particular desired frequency. This usually results in resonators whose electrodes are of different thickness. This fact also needs to be included in the analysis for an accurate description of a thin film resonator.

In this paper we perform an exact analysis of thickness vibrations of an FBAR of AlN or ZnO with tilted six-fold axis. The equations of linear piezoelectricity are used for the crystal plate. Each of the two-layered electrodes is modeled by the equations of elasticity to completely describe the mechanical effects of the electrodes, stiffness and inertia. An exact solution is obtained. Thickness vibration frequencies and modes as well as impedance are obtained. Since the structures of the material constants of polarized ceramics are the same as those of 6 mm crystals [7], the results of the present analysis also apply to piezoelectric ceramic plates with tilted poling.

2. Governing equations and solution procedure

Consider an unbounded piezoelectric plate of 6 mm crystals or polarized ceramics as shown in Fig. 1. The major surfaces of the plate are traction-free. The six-fold axis or poling direction is at an angle θ from the plate normal as indicated by the arrow P. A

* Corresponding author. Address: Department of Engineering Mechanics, University of Nebraska, Lincoln, NE 68588-0526, USA. Tel.: +1 402 472 0712; fax: +1 402 472 8292.
E-mail address: jyang1@unl.edu (J. Yang).

0041-624X/$ - see front matter © 2008 Elsevier B.V. All rights reserved.
doi:10.1016/j.ultras.2008.09.003

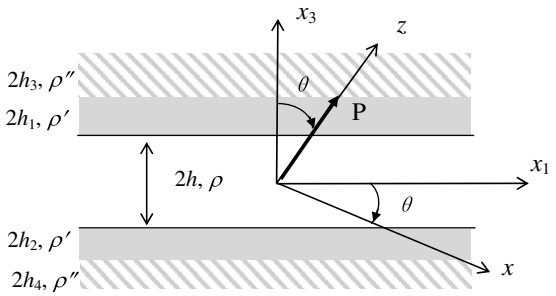

Fig. 1. A plate of 6 mm crystals with two-layered electrodes and tilted axis.

time-harmonic voltage $2V$ is applied across the electrodes. In the (x_1,x_2,x_3) system, the equations of linear piezoelectricity for the plate are written as:

$$\begin{aligned} &T_{ji,j} = \rho\ddot{u}_i, \quad D_{i,i} = 0,\\ &T_{ij} = c_{ijkl}S_{kl} - e_{kij}E_k, \quad D_i = e_{ijk}S_{jk} + \varepsilon_{ij}E_j,\\ &S_{ij} = (u_{i,j} + u_{j,i})/2, \quad E_i = -\phi_{,i}, \end{aligned} \tag{1}$$

where **u** is the mechanical displacement vector, **T** is the stress tensor, **S** is the strain tensor, **E** is the electric field, **D** is the electric displacement, ϕ is the electric potential, and ρ is the mass density. c_{ijkl}, e_{ijk} and ε_{ij} are elastic, piezoelectric and dielectric constants. The electrodes are isotropic and are modeled by the equations of linear elasticity. For the inner electrodes,

$$\begin{aligned} &T_{ji,j} = \rho'\ddot{u}_i,\\ &T_{ij} = c'_{ijkl}S_{kl},\\ &S_{ij} = (u_{i,j} + u_{j,i})/2. \end{aligned} \tag{2}$$

For the outer electrodes,

$$\begin{aligned} &T_{ji,j} = \rho''\ddot{u}_i,\\ &T_{ij} = c''_{ijkl}S_{kl},\\ &S_{ij} = (u_{i,j} + u_{j,i})/2. \end{aligned} \tag{3}$$

Under the compact matrix notation, the material tensors in Eq. (1) can be represented by matrices. In the (x,y,z) system, let the usual elastic, piezoelectric and dielectric constants of a 6 mm crystal be denoted by:

$$\begin{pmatrix} \hat{c}_{11} & \hat{c}_{12} & \hat{c}_{13} & 0 & 0 & 0\\ \hat{c}_{21} & \hat{c}_{11} & \hat{c}_{13} & 0 & 0 & 0\\ \hat{c}_{31} & \hat{c}_{31} & \hat{c}_{33} & 0 & 0 & 0\\ 0 & 0 & 0 & \hat{c}_{44} & 0 & 0\\ 0 & 0 & 0 & 0 & \hat{c}_{44} & 0\\ 0 & 0 & 0 & 0 & 0 & \hat{c}_{66} \end{pmatrix},$$
$$\begin{pmatrix} 0 & 0 & 0 & 0 & \hat{e}_{15} & 0\\ 0 & 0 & 0 & \hat{e}_{15} & 0 & 0\\ \hat{e}_{31} & \hat{e}_{31} & \hat{e}_{33} & 0 & 0 & 0 \end{pmatrix}, \tag{4}$$
$$\begin{pmatrix} \hat{\varepsilon}_{11} & 0 & 0\\ 0 & \hat{\varepsilon}_{11} & 0\\ 0 & 0 & \hat{\varepsilon}_{33} \end{pmatrix},$$

where $\hat{c}_{66} = (\hat{c}_{11} - \hat{c}_{12})/2$ and we have used a caret to distinguish them from the material constants in the indexed (1,2,3) system. By tensor transformation, for the crystal plate, c_{ijkl}, e_{kij} and ε_{ij} are related to $\hat{c}_{ijkl}$, $\hat{e}_{kij}$ and $\hat{\varepsilon}_{ij}$ by [5]:

$$\begin{aligned} c_{11} &= \cos^4(\theta)\hat{c}_{11} + 2\sin^2(\theta)\cos^2(\theta)\hat{c}_{13} + 4\sin^2(\theta)\cos^2(\theta)\hat{c}_{44}\\ &\quad + \sin^4(\theta)\hat{c}_{33},\\ c_{12} &= \cos^2(\theta)\hat{c}_{12} + \sin^2(\theta)\hat{c}_{13},\\ c_{13} &= \sin^2(\theta)\cos^2(\theta)\hat{c}_{11} + \sin^4(\theta)\hat{c}_{13} - 4\sin^2(\theta)\cos^2(\theta)\hat{c}_{44}\\ &\quad + \cos^4(\theta)\hat{c}_{13} + \cos^2(\theta)\sin^2(\theta)\hat{c}_{33},\\ c_{15} &= -\sin(\theta)\cos^3(\theta)\hat{c}_{11} - \sin^3(\theta)\cos(\theta)\hat{c}_{13} - 2\sin^3(\theta)\cos(\theta)\hat{c}_{44}\\ &\quad + 2\sin(\theta)\cos^3(\theta)\hat{c}_{44} + \sin(\theta)\cos^3(\theta)\hat{c}_{13} + \sin^3(\theta)\cos(\theta)\hat{c}_{33},\\ c_{21} &= \hat{c}_{12}, \quad c_{22} = \hat{c}_{11}, \quad c_{23} = \sin^2(\theta)\hat{c}_{12} + \cos^2(\theta)\hat{c}_{13},\\ c_{25} &= -\sin(\theta)\cos(\theta)\hat{c}_{12} + \sin(\theta)\cos(\theta)\hat{c}_{13},\\ c_{33} &= \sin^4(\theta)\hat{c}_{11} + 2\sin^2(\theta)\cos^2(\theta)\hat{c}_{13} + 4\sin^2(\theta)\cos^2(\theta)\hat{c}_{44}\\ &\quad + \cos^4(\theta)\hat{c}_{33},\\ c_{35} &= -\sin^3(\theta)\cos(\theta)\hat{c}_{11} + \sin^3(\theta)\cos(\theta)\hat{c}_{13} - 2\sin(\theta)\cos^3(\theta)\hat{c}_{44}\\ &\quad + 2\sin^3(\theta)\cos(\theta)\hat{c}_{44} - \sin(\theta)\cos^3(\theta)\hat{c}_{13} + \sin(\theta)\cos^3(\theta)\hat{c}_{33},\\ c_{44} &= 0.5\sin^2(\theta)(\hat{c}_{11} - \hat{c}_{12}) + \cos^2(\theta)\hat{c}_{44},\\ c_{46} &= -0.5\sin(\theta)\cos(\theta)(\hat{c}_{11} - \hat{c}_{12}) + \sin(\theta)\cos(\theta)\hat{c}_{44},\\ c_{55} &= \sin^2(\theta)\cos^2(\theta)\hat{c}_{11} - 2\sin^2(\theta)\cos^2(\theta)\hat{c}_{13} - 2\sin^2(\theta)\cos^2(\theta)\hat{c}_{44}\\ &\quad + (\sin^4(\theta) + \cos^4(\theta))\hat{c}_{44} + \sin^2(\theta)\cos^2(\theta)\hat{c}_{33},\\ c_{66} &= 0.5\cos^2(\theta)(\hat{c}_{11} - \hat{c}_{12}) + \sin^2(\theta)\hat{c}_{44}, \end{aligned} \tag{5}$$

$$\begin{aligned} e_{11} &= 2\sin(\theta)\cos^2(\theta)\hat{e}_{15} + \sin(\theta)\cos^2(\theta)\hat{e}_{31} + \sin^3(\theta)\hat{e}_{33},\\ e_{12} &= \sin(\theta)\hat{e}_{31},\\ e_{13} &= -2\sin(\theta)\cos^2(\theta)\hat{e}_{15} + \sin^3(\theta)\hat{e}_{31} + \sin(\theta)\cos^2(\theta)\hat{e}_{33},\\ e_{15} &= (-\sin^2(\theta)\cos(\theta) + \cos^3(\theta))\hat{e}_{15} - \sin^2(\theta)\cos(\theta)\hat{e}_{31}\\ &\quad + \sin^2(\theta)\cos(\theta)\hat{e}_{33},\\ e_{24} &= \cos(\theta)\hat{e}_{15},\\ e_{26} &= \sin(\theta)\hat{e}_{15},\\ e_{31} &= -2\sin^2(\theta)\cos(\theta)\hat{e}_{15} + \cos^3(\theta)\hat{e}_{31} + \sin^2(\theta)\cos(\theta)\hat{e}_{33},\\ e_{32} &= \cos(\theta)\hat{e}_{31}, e_{33} = 2\cos(\theta)\sin^2(\theta)\hat{e}_{15} + \cos^3(\theta)\hat{e}_{33}\\ &\quad + \cos(\theta)\sin^2(\theta)\hat{e}_{31},\\ e_{35} &= -\cos^2(\theta)\sin(\theta)\hat{e}_{31} + \cos^2(\theta)\sin(\theta)\hat{e}_{33} - \sin(\theta)(\cos^2(\theta)\\ &\quad - \sin^2(\theta))\hat{e}_{15} \end{aligned} \tag{6}$$

$$\begin{aligned} \varepsilon_{11} &= \cos^2(\theta)\hat{\varepsilon}_{11} + \sin^2(\theta)\hat{\varepsilon}_{33},\\ \varepsilon_{13} &= -\sin(\theta)\cos(\theta)\hat{\varepsilon}_{11} + \sin(\theta)\cos(\theta)\hat{\varepsilon}_{33},\\ \varepsilon_{22} &= \hat{\varepsilon}_{11},\\ \varepsilon_{31} &= -\cos(\theta)\sin(\theta)\hat{\varepsilon}_{11} + \cos(\theta)\sin(\theta)\hat{\varepsilon}_{33},\\ \varepsilon_{33} &= \sin^2(\theta)\hat{\varepsilon}_{11} + \cos^2(\theta)\hat{\varepsilon}_{33}. \end{aligned} \tag{7}$$

With successive substitutions, the equations of motion and the charge or Gauss equation of electrostatics for the crystal plate can be written as:

$$\begin{aligned} &c_{55}u_{1,33} + c_{35}u_{3,33} + e_{35}\phi_{,33} = \rho\ddot{u}_1,\\ &c_{44}u_{2,33} = \rho\ddot{u}_2,\\ &c_{35}u_{1,33} + c_{33}u_{3,33} + e_{33}\phi_{,33} = \rho\ddot{u}_3,\\ &e_{35}u_{1,33} + e_{33}u_{3,33} - \varepsilon_{33}\phi_{,33} = 0. \end{aligned} \tag{8}$$

Eq. (8) shows that u_2 is alone, representing a thickness-shear mode that is well understood and will not be considered in this paper. u_1, u_3 and ϕ represent coupled thickness-shear and thickness-stretch which we want to study. Boundary and interface continuity conditions are

$$
\begin{aligned}
&T_{31}=0, \quad T_{33}=0, \quad x_3=h+2h_1+2h_3,\\
&[u_1,u_3,T_{31},T_{33}]=0, \quad x_3=h+2h_1,\\
&[u_1,u_3,T_{31},T_{33}]=0, \quad \phi=V, \quad x_3=h,\\
&[u_1,u_3,T_{31},T_{33}]=0, \quad \phi=-V, \quad x_3=-h,\\
&[u_1,u_3,T_{31},T_{33}]=0, \quad x_3=-(h+2h_2),\\
&T_{31}=0, \quad T_{33}=0, \quad x_3=-(h+2h_2+2h_4),
\end{aligned}
\tag{9}
$$

where a field variable inside a pair of square brackets represents the jump of the variable across an interface. The free charge Q on and the current I that flows into the electrode at $x_3 = h$ are given by:

$$
\begin{aligned}
&D_3=e_{33}u_{3,3}+e_{35}u_{1,3}-\varepsilon_{33}\phi_{,3},\\
&Q=-D_3(x_3=h)S,\\
&I=\dot{Q}=i\omega Q,
\end{aligned}
\tag{10}
$$

where S is the electrode area under consideration. Then the admittance and impedance per unit area of the plate can be calculated from

$$
A=\frac{I}{2V}, \quad Z=1/A. \tag{11}
$$

The solution procedure consists of obtaining solutions for each layer and then applying the boundary and continuity conditions, which is not provided here for conciseness.

3. Numerical results

The electrodes are made from titanium and platinum, with the titanium layers in contact with the crystal plate. Titanium and platinum are isotropic materials with two independent elastic constants

$$
c_{11}=\frac{E(1-\nu)}{(1+\nu)(1-2\nu)}, \quad c_{12}=\frac{E\nu}{(1+\nu)(1-2\nu)}, \tag{12}
$$

where E is Young's modulus and ν is Poisson's ratio. For the crystal plate we consider AlN. $2h = 440$ nm, $2h_2 = 2h_1 = 15$ nm, $2h_4 = 2h_3 = 100$ nm, $S = 50 \times 50\ \mu m^2$. These data are based on [3] but comparison with [3] cannot be made because the experimental data in [3] are for a plate on a substrate. Some damping is introduced by allowing the relevant elastic material constants to assume complex values, which can represent viscous damping in the material. For example, in our calculations $\hat{c}_{33}$ is replaced by $\hat{c}_{33}\ (1 + iQ^{-1})$ where Q is a large and real number. The rest of the elastic constants are treated similarly. We fix $Q = 10^2$. $\theta = 70^\circ$. The material constants in the (x,y,z) system are

AlN:

$$
\varepsilon_0 = 8.75\times10^{-12}\ \text{F/m},\ \rho = 3512\ \text{kg/m}^3,
$$

$$
[\hat{c}_{pq}] = \begin{pmatrix} 345 & 125 & 120 & 0 & 0 & 0\\ 125 & 345 & 120 & 0 & 0 & 0\\ 120 & 120 & 395 & 0 & 0 & 0\\ 0 & 0 & 0 & 118 & 0 & 0\\ 0 & 0 & 0 & 0 & 118 & 0\\ 0 & 0 & 0 & 0 & 0 & 110 \end{pmatrix} \times 10^9\ \text{N/m}^2,
$$

$$
[\hat{e}_{ip}] = \begin{pmatrix} 0 & 0 & 0 & 0 & -0.48 & 0\\ 0 & 0 & 0 & -0.48 & 0 & 0\\ -0.58 & -0.58 & 1.55 & 0 & 0 & 0 \end{pmatrix}\ \text{c/m}^2,
$$

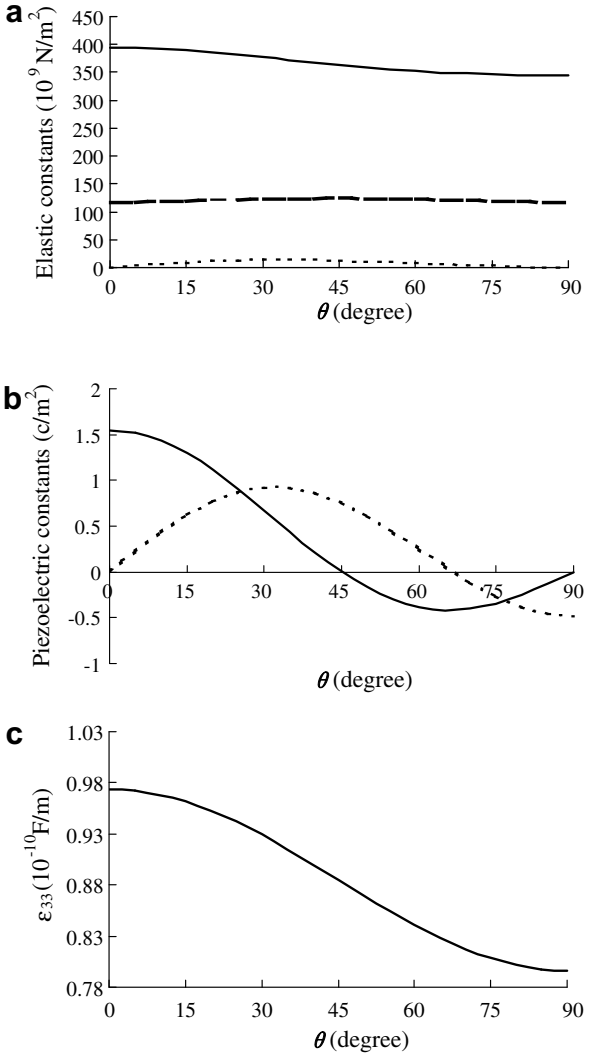

Fig. 2. Material constants of AlN. (a) Elastic constants. c_{33}, solid; c_{35}, dotted; c_{55}, dash. (b) Piezoelectric constants. e_{33}, solid; e_{35}, dotted. (c) Dielectric constant.

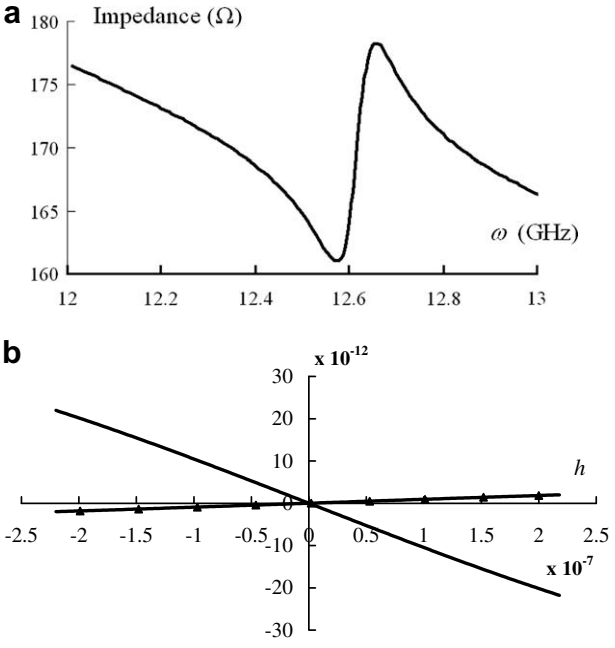

Fig. 3. First resonance (a) and the corresponding mode (b) (u_1, solid and u_3, triangle).

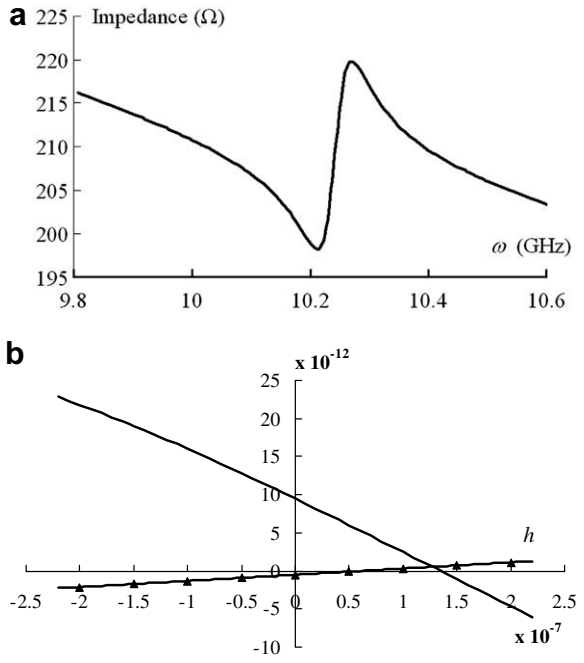

Fig. 4. Effects of electrodes of unequal thickness: (a) resonance and (b) mode (u_1, solid and u_3, triangle).

$$[\hat{\varepsilon}_{ij}] = \begin{pmatrix} 9 & 0 & 0 \\ 0 & 9 & 0 \\ 0 & 0 & 11 \end{pmatrix} \varepsilon_0.$$

Titanium:

$\rho = 4507$ kg/m^3, $E = 116$ GPa, $\nu = 0.34$.

Platinum:

$\rho = 21450$ kg/m^3, $E = 171$ GPa, $\nu = 0.39$.

We plot the relevant elastic, piezoelectric and dielectric constants in the (1,2,3) system in Fig. 2. The figure shows that the elastic constants change slowly. In particular, c_{35} is very small. Therefore in these materials the coupling between thickness-shear and thickness-stretch is weak. The piezoelectric and dielectric constants are more sensitive to the material orientation. The piezoelectric constants cross zero occasionally, indicating that for some particular values of θ a thickness electric field tends to excite a pure thickness-shear or thickness-stretch mode. Since c_{35} is very small, essentially thickness-shear or essentially thickness-stretch modes can be excited in these plates with particular values of θ. Fig. 2b was given earlier in [5] and is reproduced here for completeness.

Fig. 3 shows impedance versus driving frequency and the displacement distribution (mode shape) along the AlN plate thickness at the first resonant frequency where the impedance assumes minimum. Frequencies for which the impedance assume maximum are called anti-resonance. Only the displacements in the crystal plate are shown, without the displacements in the electrodes. From the mode shapes we can see that the first mode is thickness-shear dominant with a large u_1.

In Fig. 4 we double the upper outer platinum electrode thickness to $2h_3$ = 200 nm. The first resonance is shown, which is lower than Fig. 3a because of the additional inertia of the thicker electrode. Due to the loss of symmetry of the structure about the middle plane of the crystal plate, the nodal points (where the displacement vanishes) of the modes are no longer at the plate center. They move toward the thicker electrode as expected. The symmetry loss of the mode shapes has consequences regarding frequency stability.

4. Conclusion

In an AlN plate with tilted six-fold axis, one pure thickness-shear mode exists which is not coupled to the thickness electric field. The other thickness-shear mode is elastically coupled to the thickness-stretch mode, and they are coupled to the thickness electric field. For the coupled modes, the relevant elastic constants are not sensitive to material orientation. c_{35} is relatively small, implying that coupling between thickness-shear and thickness-stretch is usually weak. The piezoelectric and dielectric constants are sensitive to material orientation. For certain orientations a particular piezoelectric constant may vanish, in which case the thickness electric field is electrically coupled to thickness-shear only or thickness-stretch only. Plates of a few hundreds of nanometers in thickness produce multi-GHz frequencies. The corresponding modes maybe thickness-shear or thickness-stretch dominant. Unequal or asymmetric electrodes cause mode centers to shift toward the thicker electrode. Similar behavior was also observed in ZnO plates.

Acknowledgements

This research is supported by a grant from the Science and Technology Division, Zhejiang Province, China, under Key Technological Initiative Program (Project No. 2006C14021). Additional supports are from Ningbo University through the Qianjiang Fellow Fund and the Research Promotion Initiative. The last author wishes to thank the authors of [5] for the availability of [5] before it has been published. This work is also supported by the K.C.Wong Magna Fund in Ningbo University and China's National Natural Science Foundation under contract No.10772087.

References

[1] W. Pang, H. Zhang, E.S. Kim, Micromachined acoustic wave resonator isolated from substrate, IEEE Transactions on Ultrasonics, Ferroelectrics, and Frequency Control 52 (2005) 1239–1246.
[2] M. Link, M. Schreiter, J. Weber, R. Primig, D. Pitzer, R. Cabl, Solidly mounted ZnO shear mode film bulk acoustic wave resonators for sensing applications in liquids, IEEE Transactions on Ultrasonics, Ferroelectrics, and Frequency Control 53 (2006) 492–496.
[3] F. Martin, M.-E. Jan, S. Rey-Mermet, B. Belgacem, D. Su, M. Cantoni, P. Muralt, Shear mode coupling and tilted grain growth of AlN thin films in BAW resonators, IEEE Transactions on Ultrasonics, Ferroelectrics, and Frequency Control 53 (2006) 1339–1343.
[4] T. Yanagitani, N. Mishima, M. Matsukawa, Y. Yatanabe, Electromechanical coupling coefficient k_{15} of polycrystalline ZnO films with the *c*-axis lie in the substrate plane, IEEE Transactions on Ultrasonics, Ferroelectrics, and Frequency Control 54 (2007) 701–704.
[5] H.F. Zhang, J.A. Turner, J.A. Kosinski, Analysis of thickness vibrations of *c*-axis inclined aluminum–nitrogen thin film resonators, in preparation.
[6] W. Pang, H. Zhang, E.S. Kim, Analytical and experimental study on second harmonic response of FBAR for oscillator application above 2 GHz, in: Proceedings of the IEEE International Ultrasonics Symposium, vol. 4, Rotterdam, the Netherlands, September 18–21, 2005, pp. 18–21.
[7] H.F. Tiersten, Linear Piezoelectric Plate Vibrations, Plenum, New York, 1969.